Comparative analysis of slope classes and terrain ruggedness index using distinct digital elevation models in the Municipality of Jenipapo de Minas

Jorge Luiz dos Santos Gomes[1] iD

[1] Federal University of Jequitinhonha and Mucuri Valleys, Teófilo Otoni, Brazil.

Email address
jorge.gomes@ufvjm.edu.br (Jorge L.S. Gomes) – Corresponding author.

Abstract

This study assesses terrain variability in the Municipality of Jenipapo de Minas, southeastern Brazil, using Digital Elevation Models (DEMs). The DEMs analyzed include the Shuttle Radar Topography Mission (SRTM) with 30-meter (SRTM30) and 90-meter (SRTM90) resolutions, as well as the Advanced Spaceborne Thermal Emission and Reflection Radiometer (ASTER). The comparative analysis was based on topographic characteristics, such as slope and terrain ruggedness index (TRI) were derived from these models to analyze the landscape's elevation changes. Results showed that elevation differences among the DEMs were similar. The predominant slope was undulating and heavily undulating, consistent with previous studies. The TRI results indicated a high incidence of level terrain, particularly in SRTM30 with 100% of the area and ASTER with almost 100%. However, in the SRTM90, the incidence of the nearly level and slightly Rugged TRI classes in 6.88% of the study area. These findings emphasize how DEM resolution influences terrain characterization, with implications for hydrological studies, environmental planning, and landscape management. Overall, the study underscores the necessity of carefully selecting DEM sources according to the specific analytical requirements, as well as the potential for using a combination of DEMs for a more comprehensive understanding of terrain dynamics across different spatial scales.

Keywords: Aster GDEM, SRTM, TRI, Topography characteristics.

1. Introduction

Terrain ruggedness is a critical metric in geospatial analysis, reflecting the variability in elevation and the complexity of the landscape. It impacts ecological patterns, hydrological processes, and land use management. The terrain ruggedness index (TRI), originally proposed by Riley, DeGloria and Elliott (1999), measures the heterogeneity of elevation, aiding in understanding the topography's influence on environmental processes (Brožová et al., 2021; Okolie and Smit, 2022).

In the municipality of Jenipapo de Minas, located in southeastern Brazil (Figure 1), terrain variability influences land use, soil stability, and water flow patterns. The use of Digital Elevation Models (DEMs) such as the Shuttle Radar Topography Mission (SRTM) at 30-meter (SRTM30) and 90-meter (SRTM90) resolutions, along with the Advanced Spaceborne Thermal Emission and Reflection Radiometer (ASTER), offers varying scales of topographic data. These DEMs offer varied spatial resolutions, which influence the precision and quality of TRI calculations (Thomas et al., 2014).

The first study regarding the morphometric analysis of the municipality was done by Gomes and Gomes (2015). They used SRTM 1 arc second version 3 to extract the slope and aspect information from the DEM. Since then, the official area of the study area has been updated. Furthermore, no comparative results were achieved regarding different DEMs besides the SRTM. Furthermore, a hypsometric map of the municipality can be seen in Gomes, Vieira and Hamza (2018) and they brief discussions of the hydrogeological and geological characteristics, highlighting that the rock formations are predominantly formed by the Salinas formation of the Macaúbas Group and also, the presence of tertiary plateau surfaces in the study area.

The study was conducted in Jenipapo de Minas, characterized by its varying topography ranging from low-lying plains to a few mountainous areas (Gomes and Gomes, 2015). The region's diverse landscape, including valleys, hills, and plateaus, makes it ideal for studying topographic heterogeneity. In this context, the present study aims to compare the terrain ruggedness index using distinct digital elevation models in the study area, as well as the influence of the chosen DEMs in the slope classification relief classes proposed by the Brazilian Agricultural Research Corporation (Embrapa, 1979).
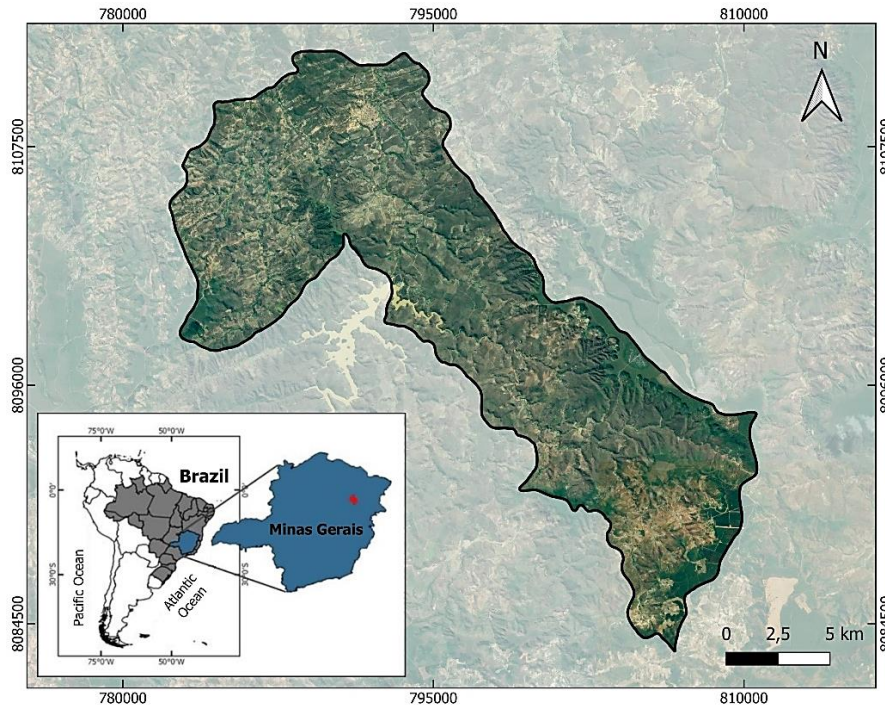

Figure 1 – Location of the Municipality of Jenipapo de Minas.

2. Methodology

Regarding the analysis of the topographical characteristics of the study area, specifically focusing on the slope and terrain ruggedness index (TRI) was utilized Shuttle Radar Topography Mission (SRTM) of 1 and 3 arc-seconds (approximately 30 and 90 meters, respectively) and Advanced Spaceborne Thermal Emission and Reflection Radiometer (ASTER) datasets. Both SRTM and ASTER provide high-resolution digital elevation models (DEMs) essential for deriving slope and terrain ruggedness.

To ensure comparability between the datasets, preprocessing steps included reprojecting ASTER and SRTM data to match the local projection system (SIRGAS 2000). After this, the slopes and TRIs were calculated and reclassified, thematic maps were created for each of the variables and DEMs used. Finally, the data from each layer created was exported for analysis to allow a comparison of the results obtained.

2.1. Digital Elevation Models (DEMs)

All the digital elevation modes (DEMs) chosen, after geoprocessing were reclassified into seven classes as shown in Table (1), for the generation of thematic maps and statistical analysis.

Table 1 – Range of the elevation classes adopted on reclassification of the DEMs.

Classes	Elevation (m)
1	< 400
2	400 – 500
3	500 – 600
4	600 –700
5	700 – 800
6	800 – 900
7	> 900

2.1.1. SRTM Elevation Model and its Derivations

The SRTM elevation model offers near-global coverage and an open digital elevation data

collection. Conducted by NASA and the National Geospatial-Intelligence Agency (NGA) in 2000, the SRTM utilized interferometric synthetic aperture radar (InSAR) technology to capture elevation data (Passini and Jacobsen, 2007) for more than 80% of Earth's landmass (Nikolakopoulos, Kamaratakis and Chrysoulakis, 2006; Ouerghi et al., 2015). SRTM derived products, such as SRTM30 and SRTM90 models, remain indispensable in geospatial analyses (Van Zyl, 2001), providing essential data for disciplines ranging from ecology (Moudrý et al., 2018; Silva, Gomes and Oliveira, 2023; Dian et al., 2024) and geology (Rossetti and Valeriano, 2007; EL-Omairi, Garouani and Shebl, 2024) to urban planning and hydrology (e.g., Cunha and Bacani, 2016; Arabameri et al., 2020; Gomes, 2020; Dell'Acqua and Gamba, 2002).

The SRTM mission used radar interferometry with two radar antennas spaced apart to create 3D elevation data. The mission elevation data, initially collected in 1-arc-second (~30m) and 3-arc-second (~90m) resolutions, has since been refined through processing to produce accurate and seamless elevation models across diverse terrains (Farr et al., 2007). As previously mentioned, SRTM data is commonly available in two key derivatives:

- SRTM90 (3-arc-second resolution, ~90m): It provides a broader view suitable for regional-scale analyses where finer topographic detail is less critical (Farr et al., 2007). This model is advantageous for extensive geological studies, climate research, and large-scale environmental assessments. Because of its lower resolution, SRTM90 smooths out smaller terrain variations but remains effective for capturing overall terrain trends in larger regions (Jarvis et al., 2008). For example, in low-relief areas with heterogeneous vegetation, SRTM may not accurately represent subtle elevation changes and can even produce an "inverted terrain model" where forested areas appear higher than surrounding agricultural land (Rodríguez et al., 2006; Lalonde et al., 2010).
- SRTM30 (1-arc-second resolution, ~30m): This high-resolution model offers detailed elevation data, making it ideal for studies requiring more precise topographic information than SRTM90, such as ecological modeling, urban planning, and localized hydrological assessments. For instance, one

study demonstrates that SRTM3 data can represent terrain variations adequately, particularly in mountainous regions where high-resolution DEMs like SRTM are crucial for accurate geomorphological analysis (Denker, 2005). Additionally, SRTM30 and its derivative products are praised for providing consistent terrain features across various landscapes, from rolling hills to steep mountain slopes, with suitable accuracy for mid-scale analysis (Liu et al., 2020).

2.1.2. ASTER Global Digital Elevation Model

The Advanced Spaceborne Thermal Emission and Reflection Radiometer (ASTER) Global Digital Elevation Model (GDEM) is a high-resolution elevation dataset produced through collaboration between NASA and Japan's Ministry of Economy, Trade, and Industry (METI). ASTER GDEM provides near-global coverage at 30-meter spatial resolution, offering valuable insights for various applications including hydrology (Thakuri et al., 2022; AL-Areeq et al., 2023), geology (Asran, Emam and El-Fakharani, 2017), ecology (Moudrý et al., 2018), and urban planning. Since its first release in 2009 (Ouerghi et al., 2015), ASTER GDEM has been widely used in terrain analysis, particularly in mountainous and remote areas where high-resolution topographic data are essential but often limited.

ASTER, a sensor onboard NASA's Terra satellite launched in 1999, collects multispectral images, including near-infrared data, which allows for stereoscopic (3D) imaging. By capturing stereo-pairs of images over the same area, ASTER GDEM generates digital elevation models through photogrammetric techniques. ASTER GDEM's unique feature is its near-global coverage between latitudes 83°N and 83°S, allowing access to topographic data even in high-latitude regions where other DEM sources like the Shuttle Radar Topography Mission (SRTM) are limited (Abrams, 2010; Liu et al., 2020; Uuemaa et al., 2020).

2.2. Slope classes

The declivity data were divided into six new classes according to the classification proposed by Embrapa (1979). According to this proposal, the classes are distributed in 0-3% (flat or almost flat), 3-8% (gently-undulating), 8-20% (undulating), 20-

45% (heavily-undulating), 45-75% (hilly) and greater than 75% (Steep). The names of each class were adapted to meet (in general) the landscape unit classifications of Van Zuidam and van Zuidam-Cancelado (1979), Van Zuidam (1983), and also the proposed classification of Listyani (2019), as used by Gomes (2020) and shown in Table (2).

Table 2 – Slope classes adapted from Embrapa (1979).

Classes	Slope (Relief)
1	Flat or almost flat (0 – 3%)
2	Gently-Undulating (3 – 8%)
3	Undulating (8 – 20%)
4	Heavily-Undulating (20 – 45%)
5	Hilly (45 – 75%)
6	Steep (Mountainous) (> 75%)

2.3. Terrain Ruggedness Index Calculation

TRI is calculated based on elevation data derived from digital elevation models (DEMs). This index is designed to quantify elevation variation by examining the altitude changes over specific areas. The calculation involves summing the absolute elevation differences between a focal cell and its adjacent cells, divided by the number of neighbors. This flexible method allows adaptation for different scales, resolutions, and topographic structures (Riley, DeGloria and Elliott, 1999). The equation (1) for TRI is

$$TRI = \sum_{i=1}^{n} \frac{|Z_{central} - Z_{neighbor,i}|}{n} \quad (1)$$

where $Z_{central}$ is the elevation of the central cell, $Z_{neighbor,i}$ is the elevation of the neighboring cell, and n is the number of neighbors.

In the present analysis, TRI calculations were performed using a 3x3 window size to maintain consistency across all DEMs, as exemplified by Riley, DeGloria and Elliott (1999). TRI was calculated by measuring the elevation differences between a central cell and its surrounding cells (e.g. Vukomanovic and Orr, 2014) using a rolling window technique (Bifet and Gavaldà, 2007; Shen et al., 2021). For this, the software *QGIS* (version 3.34.6) was utilized to automate the process, and the results were analyzed for comparing the TRI values derived from each DEM.

The declivity data were divided into seven classes according to the classification proposed by Riley, DeGloria and Elliott (1999), as shown in Table (3).

Table 3 – Terrain ruggedness index categories.

Classes	Category / Elevation Difference (m)
1	Level (0 – 80)
2	Nearly Level (81 – 116)
3	Slightly Rugged (117 – 161)
4	Intermediately Rugged (162 – 239)
5	Moderately Rugged (240 – 497)
6	Highly Rugged (498 – 958)
7	Extremely Rugged (959 – 4367)

3. Results and discussion

The results of the comparative analysis of elevation, slope, and the terrain ruggedness index based on distinct digital elevation models in the Municipality of Jenipapo de Minas are shown in Tables (4 to 13) and Figures (2 to 13).

The official area of the municipality according to IBGE (2022a) is 284.45 km². However, in the context of distinct raster files (DEMs) with different spatial resolutions, the calculated area was 284.86, 284.73, and 284.82 km² for SRTM30, SRTM90, and ASTER, respectively.

Regarding the elevation from the DEMs used, all data were reclassified for statistical analysis and an area count (in km²) was performed for each class, as shown in Tables (4 to 6) and Figure (2). After, as a final procedure, hypsometric (elevation) maps were prepared for the study area, as illustrated in the reclass map in Figure (3) and hypsometric map in Figure (4).

The elevation class 7 has the smallest area, as a percentage of the total area, with an average value of 2.37% among DEMs. It also represents the highest regions of the municipality reaching up to 900 m in height.

Table 4 – Elevation classes with area values for SRTM30.

Classes	Elevations (m)	Area (Km²)	%
1	< 400	17.64	6.19
2	400 – 500	80.21	28.16
3	500 – 600	73.52	25.81
4	600 – 700	42.35	14.87
5	700 – 800	33.44	11.74
6	800 – 900	30.73	10.79
7	> 900	6.97	2.45
Total		**284.86**	**100**

Table 5 – Elevation classes with area values for SRTM90.

Classes	Elevations (m)	Area (Km²)	%
1	< 400	17.63	6.19
2	400 – 500	81.12	28.49
3	500 – 600	73.33	25.75
4	600 – 700	41.89	14.71
5	700 – 800	32.85	11.54
6	800 – 900	31.30	10.99
7	> 900	6.61	2.32
Total		**284.73**	**100.00**

Table 6 – Elevation classes with area values for ASTER.

Classes	Elevations (m)	Area (Km²)	%
1	< 400	23.17	8.14
2	400 – 500	80.44	28.24
3	500 – 600	70.84	24.87
4	600 – 700	41.19	14.46
5	700 – 800	32.60	11.45
6	800 – 900	29.89	10.50
7	> 900	6.67	2.34
Total		**284.82**	**100.00**
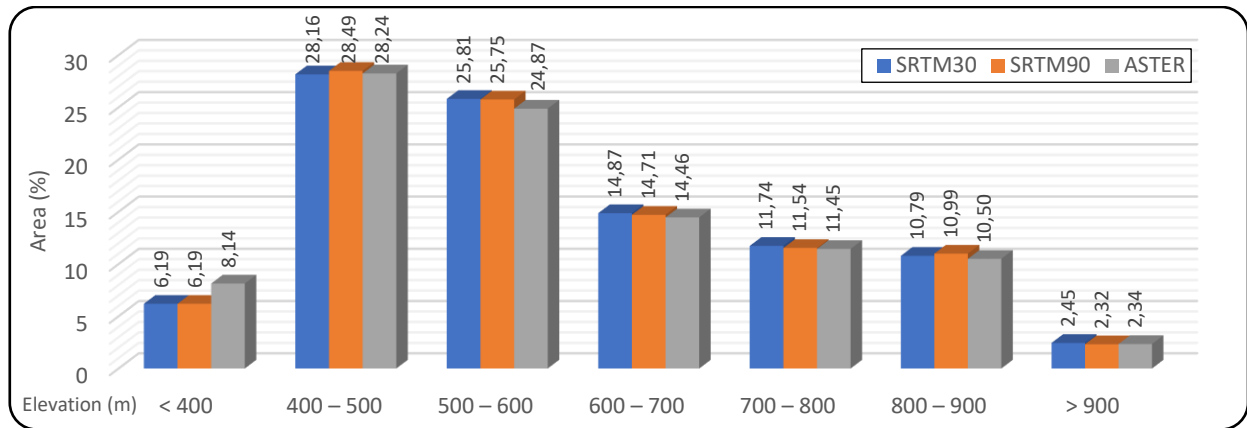
Figure 2 – Percentage distribution of the elevation classes in each DEM.
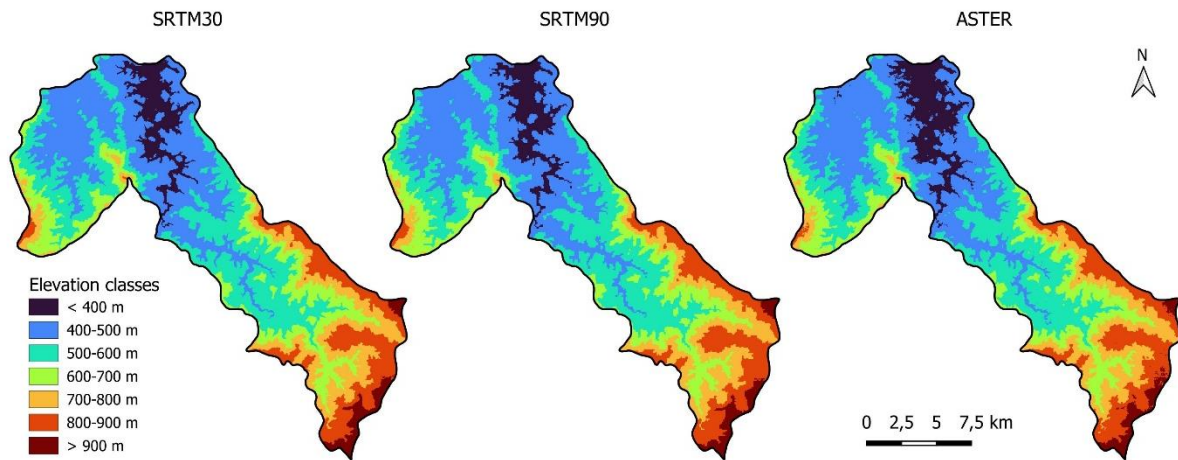

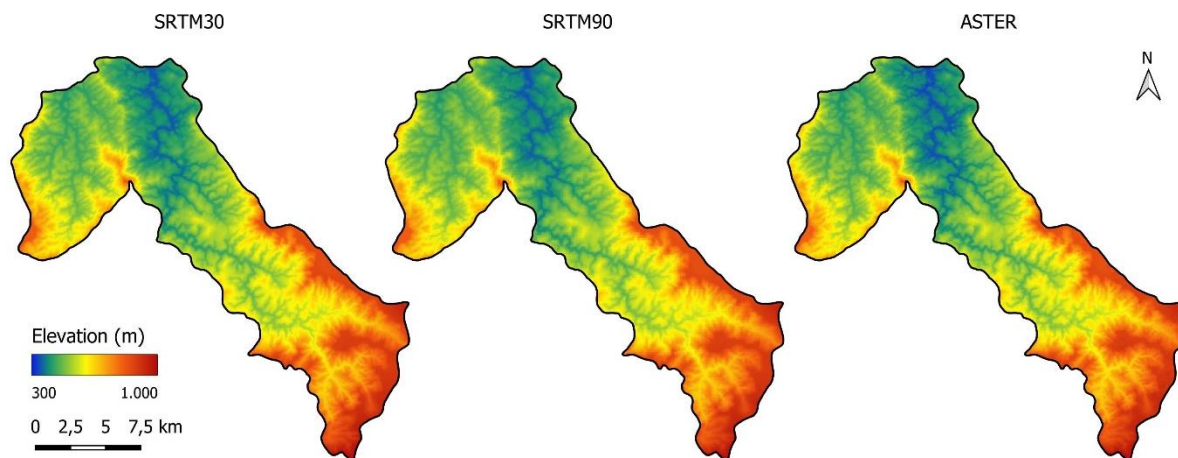Figure 3 – Elevation map with reclassified DEMs data.

Figure 4 – Hypsometric map for each DEM.

Note that the difference between the DEMs by class did not exceed 1% in all cases, except in class 1, between the SRTMs and ASTER which reached a difference of 1.95%.

Regarding the DEMs, as indicated in the reclassification data, the changes in the reclassified map (Figure 3) were minor in low-lying regions (in dark blue color), as noted in the ASTER map. Nevertheless, in the higher altitude regions (reddish colors) at the extreme east, south, and west of the reclassified and hypsometric maps is very difficult to notice any significant change.

It was not possible to note significant changes even when comparing the elevation map elaborated by Gomes and Gomes (2023a) that used NASADEM data and another color scale.

The slopes were divided into six classes and the results for each DEM are shown in Tables (7 to 9) and illustrated in Figures (5 to 8). The slope classes 3 (undulating relief) and 4 (heavily undulating relief) were predominant among the other classes, covering an average of 42.24% (120.29 km²) and 39.17% (111.57 km²) of the total area of the municipality, respectively.

Table 7 – SRTM30 slope classes by area percentage.

Classes	Slope (%)	Area (Km²)	%
1	0 – 3	12.40	4.35
2	3 – 8	32.86	11.54
3	8 – 20	107.05	37.58
4	20 – 45	123.46	43.34
5	45 – 75	9.05	3.18
6	> 75	0.04	0.01
Total		**284.86**	**100**

Table 8 – SRTM90 slope classes by area percentage.

Classes	Slope (%)	Area (Km²)	%
1	0 – 3	12.43	4.37
2	3 – 8	42.35	14.88
3	8 – 20	142.12	49.91
4	20 – 45	87.32	30.67
5	45 – 75	0.51	0.18
6	> 75	0.00	0.00
Total		**284.73**	**100**

Table 9 – ASTER slope classes by area percentage.

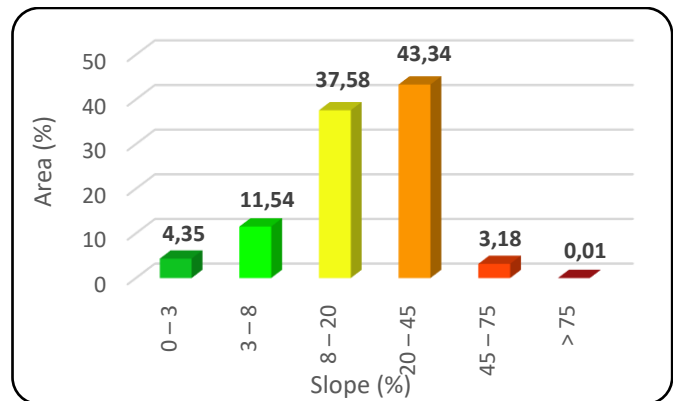| Classes	Slope (%)	Area (Km²)	%
1	0 – 3	4.59	1.61
2	3 – 8	29.78	10.46
3	8 – 20	111.72	39.22
4	20 – 45	123.93	43.51
5	45 – 75	14.57	5.11
6	> 75	0.23	0.08
Total		**284.82**	**100**

Figure 5 – Percentage of slope classes in SRTM30.
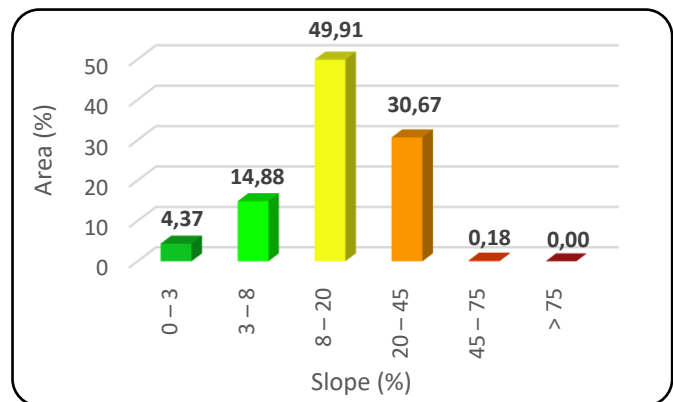

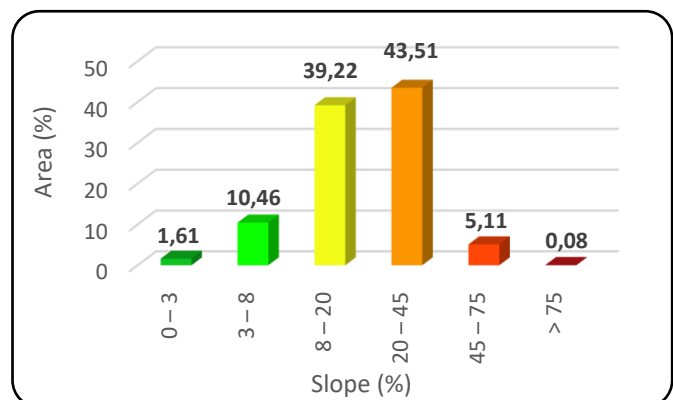Figure 6 – Percentage of slope classes in SRTM90.

Figure 7 – Percentage of slope classes in ASTER.

The slope classes showed a predominance of areas with a slope of 6 to 20% (with undulating and strongly undulating relief). As expected, the previous study of Gomes and Gomes (2015) also indicated that both classes had predominance in the area. The main difference is in the highest class 6 (steep relief) since the authors did not reveal the presence of this relief previously. However, the present study noticed the presence of class 6 in the DEMs SRTM30 and ASTER. This change was due to the update of the *shapefile* of Brazilian municipalities carried out by IBGE (2022b) a few years ago.

Furthermore, Gomes and Gomes (2023b) made three different reclassified slope maps according to Embrapa (1979), Lepsch (1991), and with a fixed interval of 10% between each class. The authors used the NASADEM data. It was possible to note that the interval chosen in the reclassification can significantly change the visualization of the map, giving the impression that the smaller the interval, the better the visual detail of the map.
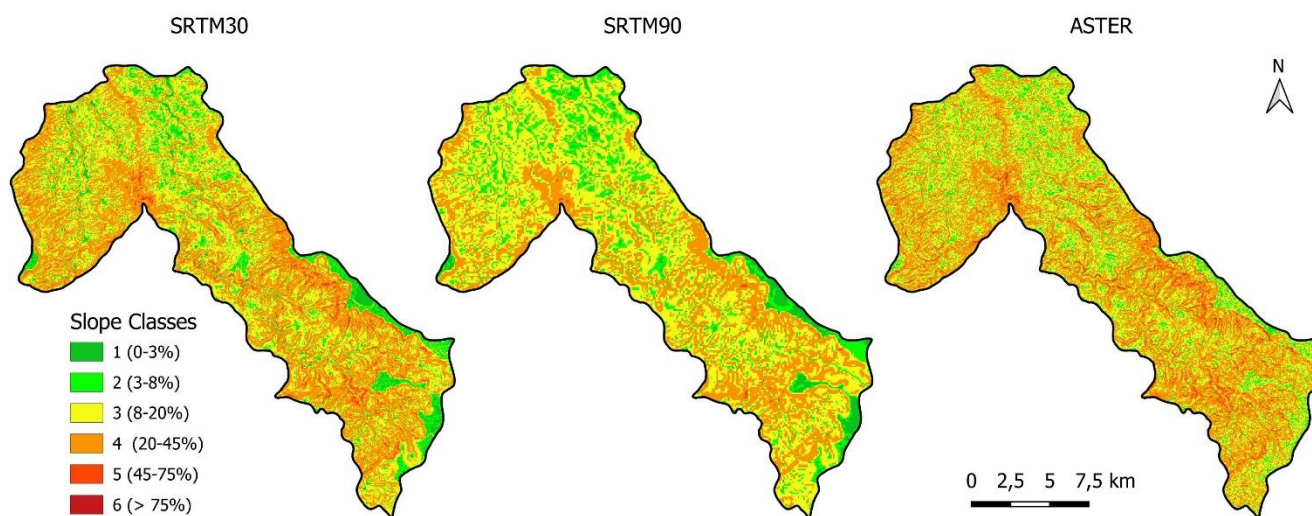

Figure 8 – Slope map according to the relief classes for the three DEMs.

The terrain ruggedness index (TRI) classification results are shown in Tables (10 to 12) and illustrated in Figures (9 to 10). The tables contain the values of each class by area and percentage of the total area. According to the results obtained, class 1, category-level terrain, has a high predominance area in all DEMs used.

In terms of percentage of the total area, the SRTM30 had 100% (Table 10) of the area in class 1, SRTM90 had 97,58% (Table 11), and ASTER got almost 100% (Table 12).

Based on SRTM90, the second class (nearly level) is present in 2.38% of the area and only 0.00256% based on ASTER.

Table 10 – SRTM30 TRI classes by area percentage.

Category / Elevation Difference (m)	Area (Km²)	%
Level (0 – 80)	284.86	100
Nearly Level (81 – 116)	0.00	0.00
Slightly Rugged (117 – 161)	0.00	0.00
Intermediately Rugged (162 – 239)	0.00	0.00
Moderately Rugged (240 – 497)	0.00	0.00
Highly Rugged (498 – 958)	0.00	0.00
Extremely Rugged (959 – 4367)	0.00	0.00
Total	**284.86**	**100**

Table 11 – SRTM90 TRI classes by area percentage.

Category / Elevation Difference (m)	Area (Km²)	%
Level (0 – 80)	277.85	97.58
Nearly Level (81 – 116)	6.77	2.38
Slightly Rugged (117 – 161)	0.11	0.04
Intermediately Rugged (162 – 239)	0.00	0.00
Moderately Rugged (240 – 497)	0.00	0.00
Highly Rugged (498 – 958)	0.00	0.00
Extremely Rugged (959 – 4367)	0.00	0.00
Total	**284.73**	**100**

Table 12 – ASTER TRI classes by area percentage.

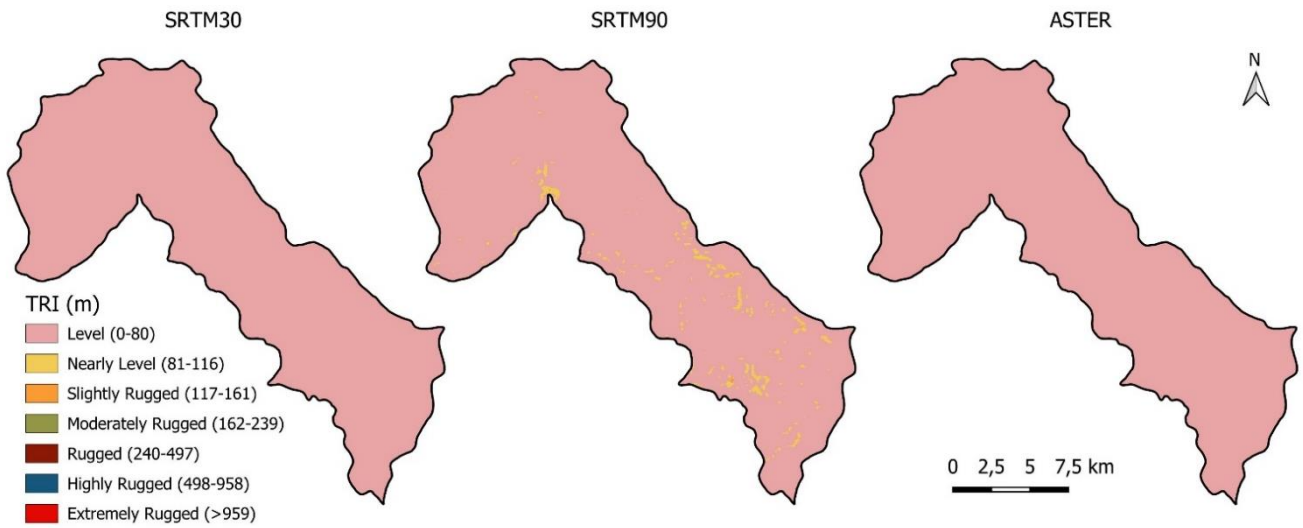| Category / Elevation Difference (m)	Area (Km²)	%
Level (0 – 80)	284.81	100
Nearly Level (81 – 116)	0.01*	0.00**
Slightly Rugged (117 – 161)	0.00	0.00
Intermediately Rugged (162 – 239)	0.00	0.00
Moderately Rugged (240 – 497)	0.00	0.00
Highly Rugged (498 – 958)	0.00	0.00
Extremely Rugged (959 – 4367)	0.00	0.00
Total	**284.82**	**100**

* 0.007293   ** 0.00256058849900493

Figure 9 – TRI map according to the Riley, DeGloria and Elliott (1999) classes for the three DEMs.
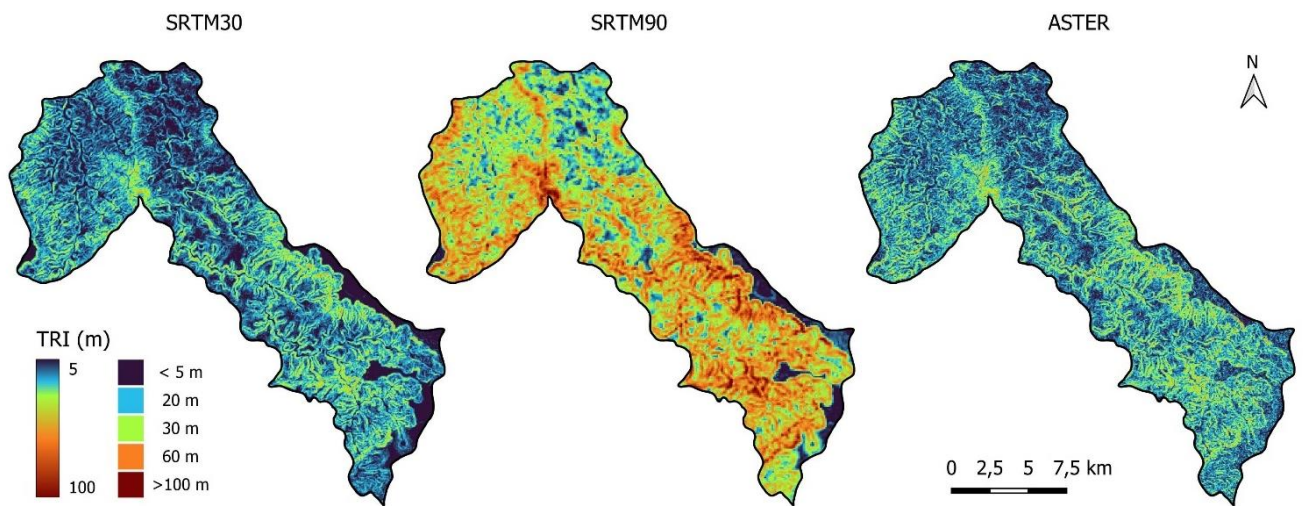

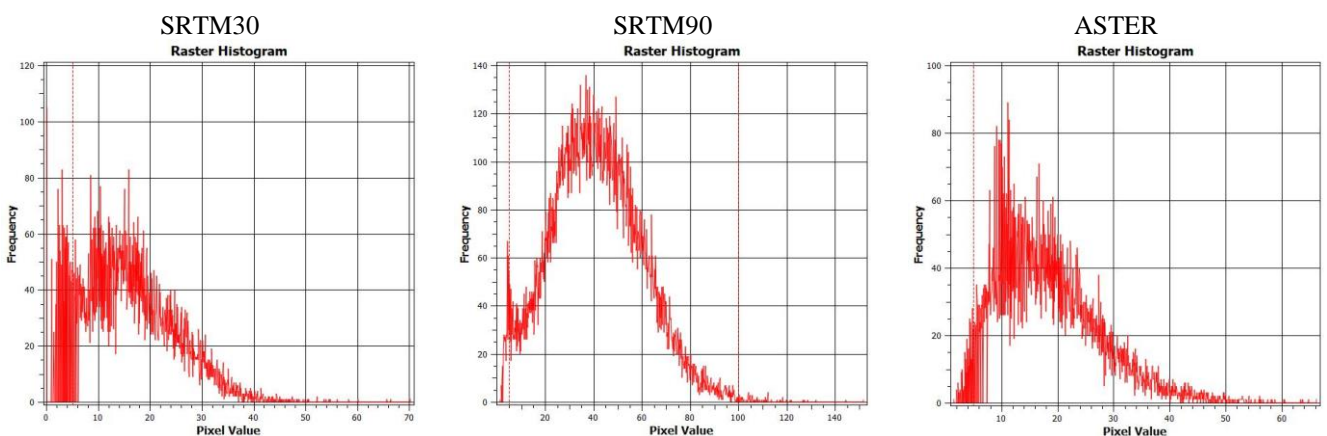Figure 10 – TRI map (classless) for the three DEMs.

Figure 11 – Histogram of each TRI.

In the TRI classified maps (Figure 9) there is homogeneity due to the predominance of class 1 (cinnamon rose color), as already pointed out in the percentage tables by class area. However, in SRTM 90 it was possible to identify the presence of class 2 (yellow color) and 3 (orange color), even in small areas. Due to the homogeneity in the classification, new TRI maps were created for the DEMS, but not classified according to Riley, DeGloria and Elliott (1999) to allow a better visual comparison of the

roughness of the study area. This provided a greater contrast between the DEMs highlighting the difference between them, mainly in SRTM90.

Analyzing the results of the TRI based on the histograms of each DEM (Figure 11):

- ASTER TRI Histogram: the frequency distribution shows a steep rise in lower TRI values, which suggests that a large portion of the terrain exhibits minimal elevation changes, characteristic of flatter or gently undulating surfaces. The histogram then gradually decreases in frequency, with fewer occurrences of higher TRI values, representing increasingly rugged terrain areas, such as heavily undulating or highly variable elevation zones. However, in most of the area, the TRI classification adopted indicates that the terrain is mostly composed of low-variability features.

- SRTM30 TRI Histogram: the histogram shows a similar pattern of lower TRI values being more frequent, but with a slightly wider spread compared to the ASTER histogram. The distribution tails off at 70 m of TRI, with minimal occurrences, reinforcing that there is no extreme ruggedness or that the spatial resolution of 30 meters smooths over finer rugged details, revealing a terrain predominantly characterized by gentle to moderate elevation variability.

- SRTM 90 TRI Histogram: the histogram differs from the other two by showing a peak at higher TRI values compared to both ASTER and SRTM30 data. The broader range of high-frequency pixel values indicates that this "coarser" spatial resolution captures more generalized ruggedness, smoothing over smaller elevation variations and highlighting broader undulations or terrain features. Consequently, the distribution suggests a terrain with moderate to substantial ruggedness levels over larger spatial extents. Even though this, concerning the TRI classification only 6.88% of the area was classified as nearly level or slightly rugged. The decline in frequency at high TRI values is more gradual, reflecting that the 90-meter resolution has aggregated areas of varied ruggedness into fewer, more generalized

categories, making rugged terrain features more prominent compared to the finer details seen in ASTER and SRTM30.

In the context of TRI, recent advancements in remote sensing technologies, such as LiDAR, have enhanced the accuracy of TRI (Trevisani, Teza and Guth, 2023) by improving DEM resolution (Esin et al., 2021). Compared to other DEMs like SRTM and LiDAR, ASTER GDEM's resolution and global coverage offer advantages, especially in high-latitude areas beyond SRTM's extent. However, ASTER's data noise is more pronounced than SRTM's, particularly in flat areas where artifacts can appear as false elevation changes. LiDAR, while generally more accurate, is not available for global coverage, making ASTER a practical alternative in remote areas lacking detailed topographic data (Suwandana et al., 2011; Mendonça and Paz, 2022).

Summarizing some previous data (Table 13), each dataset was assessed for its minimum and maximum values of elevation (in meters), slope (in percentage), and Terrain Ruggedness Index (TRI, in meters), providing insight into the topographic variability across different spatial resolutions. The elevation range for the SRTM30 extends from a minimum of 346 meters to a maximum of 978 meters, while the SRTM90 dataset covers a broader range, extending from 341 to 1003 meters. The ASTER dataset reveals a similar scope, with elevations ranging between 337 and 982 meters. These differences in elevation data highlight potential discrepancies arising from DEM resolution, as higher resolution DEMs, such as SRTM30, tend to capture localized variations in elevation more precisely than coarser-resolution models.

For SRTM30 slopes in Table (13), values range from 0% to 96.43%. The SRTM90 dataset, however, shows a reduced maximum slope of 65.71%, suggesting that "coarser" resolutions may smooth out high-gradient areas, potentially underestimating local steepness. The ASTER data is similar to SRTM30 in slope extremes, and records a maximum of 91.01%, emphasizing that higher resolution DEMs can better represent topographic feature transitions.

In terms of terrain ruggedness, the TRI values varied notably across the datasets. The SRTM30 dataset exhibits TRI values between 0 and 70.34 meters. In contrast, SRTM90 ranges more widely,

from a minimum of 1 meter to a maximum of 151.86 meters, potentially capturing broader variations in terrain due to different spatial resolutions. ASTER data, with TRI values between 1.41 and 66.26 meters, is similar to the SRTM30 range, indicating that high-resolution data are more sensitive to detecting fine-scale terrain irregularities.

In order to better visualize and compare the different DEMs and their derivatives, was created a profile (southeast to northeast) in the highlands of the municipality, as shown in Figure (12). The profile location was chosen since it crosses two local streams approximately 2000 and 6500 m away from the beginning of the profile and also passes through two flat areas. In both flattened areas, SRTM30 and ASTER showed lower oscillation compared to SRTM90, as shown in TRI, elevation, and slope profile. This profile behavior corroborates

with the histogram discussion that SRTM90 smooths out smaller terrain variations but remains effective for capturing overall terrain trends in larger regions. Furthermore, the small maps show the ASTER image in Figure (13).

Aiming to compare the thematic maps created and high-resolution satellite images, such as Bing and Google, for each DEM used. An area of relief transition from a flat to a mountainous slope was selected, the same region presented the highest (>100m) TRI values, as shown in Figure (13). In addition to the relief transition, it was possible to observe some geomorphological features, such as the drainage lines (thalweg) well characterized by the fit of relief in small valleys, the lateral continuity of the cliffs with a slight softening of the relief in the center. This variation coincides with what was observed in the TRI and slope.

Table 13 – Summary of minimum and maximum values of the variables.

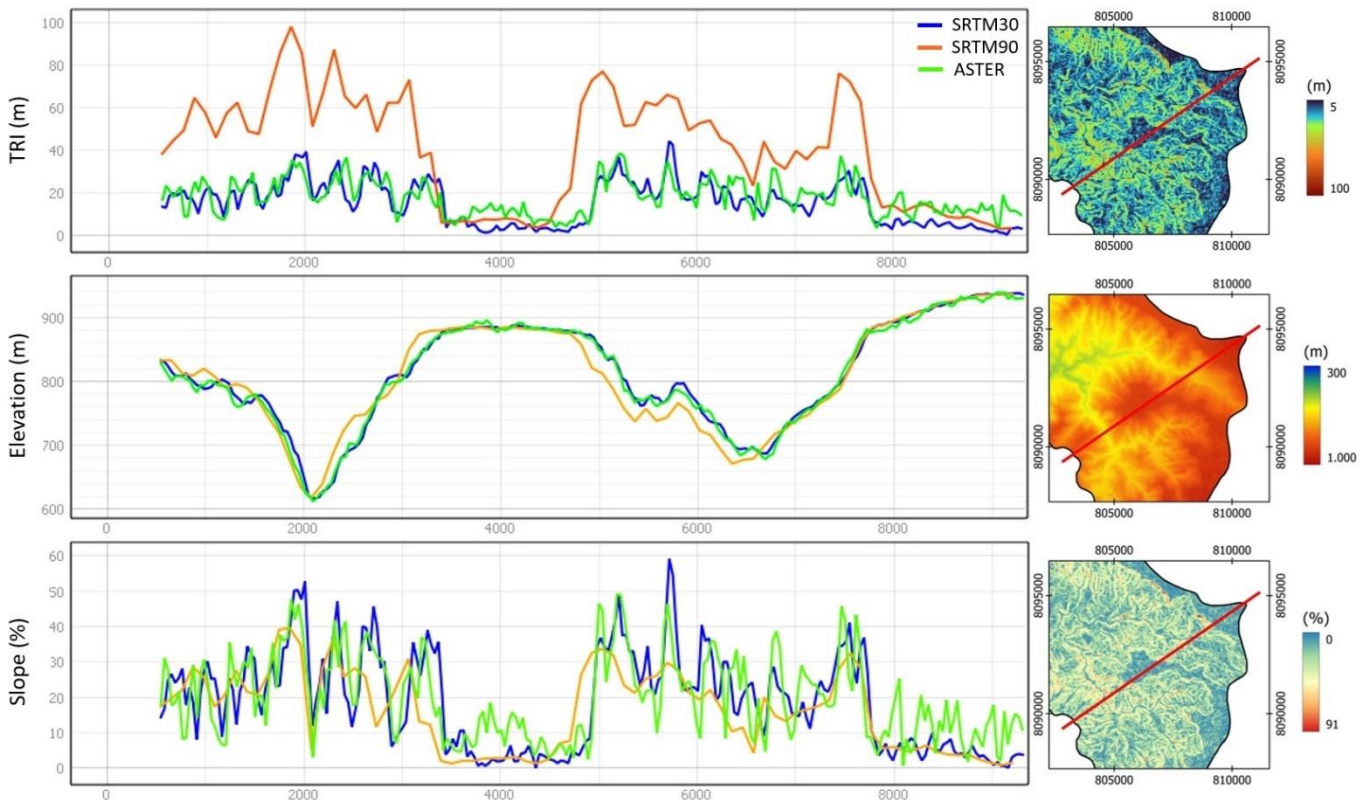| DEMs	Elevation (m)		Slope (%)		TRI (m)	
	Min.	Max.	Min.	Max.	Min.	Max.
SRTM30	346	978	0	96.43	0	70.34
SRTM90	341	1003	0	65.71	1	151.86
ASTER	337	982	0	91.01	1.41	66.26

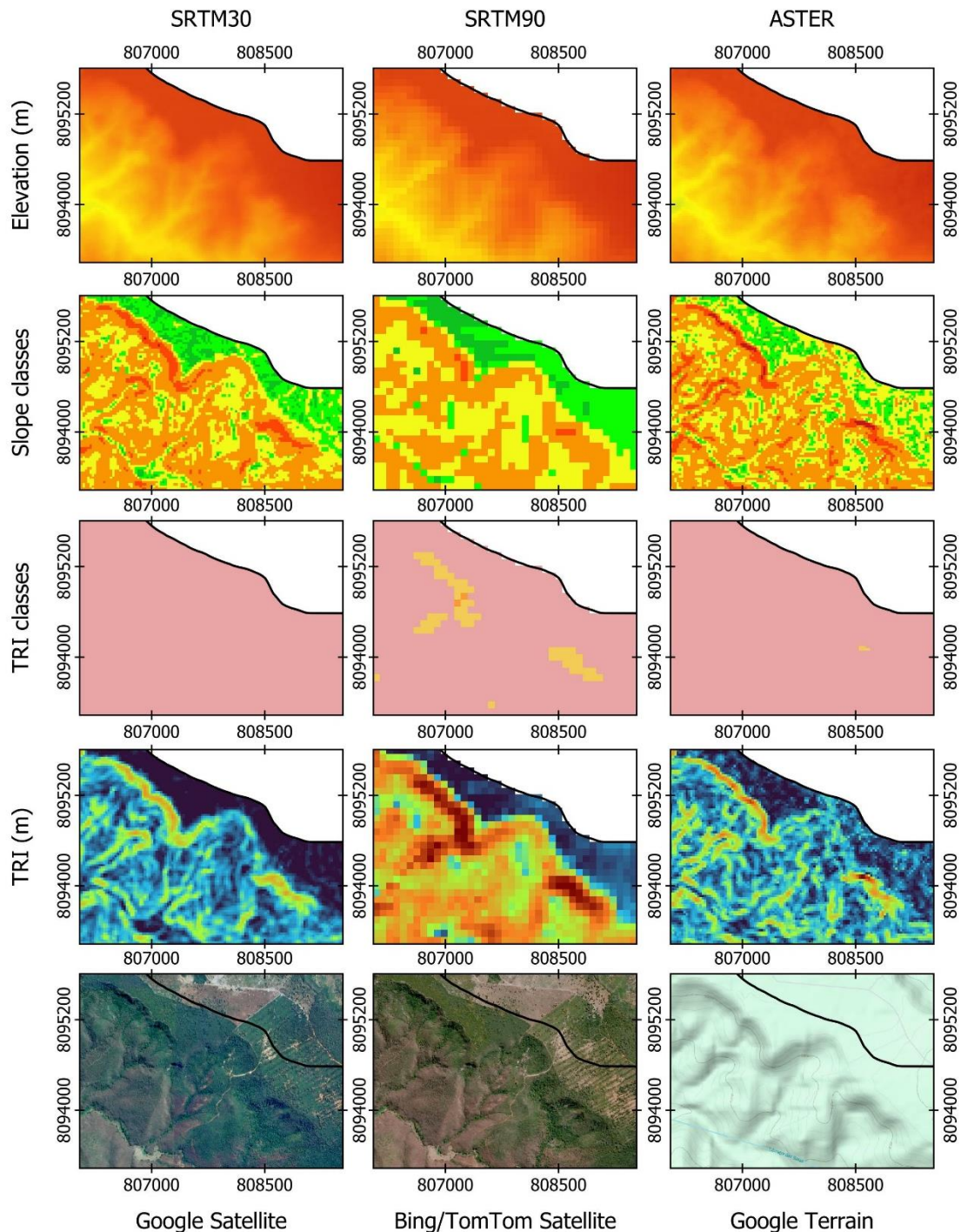Figure 12 – TRI, elevation, and slope profiles for each DEM.

Figure 13 – Comparison between different images for a region of abrupt relief variation.

6. Conclusion

Based on the detailed analysis of terrain ruggedness and slope variability across the selected digital elevation models, the present study highlights the topographical complexity in the municipality Jenipapo de Minas, demonstrating how distinct spatial resolutions influence the representation of elevation, slope, and the terrain ruggedness index. The comparison between SRTM and ASTER models reveals that while higher-resolution DEMs, such as SRTM30 offer finer coarseness in ruggedness features, the "coarser" SRTM90 still provides substantial insights for broader-scale analysis. ASTER, meanwhile, balances resolution and coverage but with noted limitations in flatter regions where minor artifacts may affect TRI calculations.

The implications of these findings extend to various environmental and planning applications, from land use management to hydrological modeling, where the choice of DEM resolution can

significantly impact the assessment of terrain characteristics. Future research could explore integrating higher-resolution data sources, such as LiDAR, to further validate and enhance terrain analyses in regions with similar geographical characteristics.

7. Acknowledgments

References

Abrams, M., Bailey, B., Tsu, H. and Hato, M., 2010. *The ASTER Global DEM*. Photogrammetric Engineering and Remote Sensing, 76(4), pp. 344-348.

AL-Areeq, A.M., Sharif, H.O., Abba, S.I., Chowdhury, S., Al-Suwaiyan, M., Benaafi, M., Yassin, M.A. and Aljundi, I.H., 2023. *Digital elevation model for flood hazards analysis in complex terrain: Case study from Jeddah, Saudi Arabia*. International Journal of Applied Earth Observation and Geoinformation, 119, p. 103330. https://doi.org/10.1016/j.jag.2023.103330

Arabameri, A., Tiefenbacher, J.P., Blaschke, T., Pradhan, B. and Bui, D.T., 2020. Morphometric Analysis for Soil Erosion Susceptibility Mapping Using Novel GIS-Based Ensemble Model. Remote sesing 12, p.874. https://doi.org/10.3390/rs12050874

Asran, A.M., Emam, A. and El-Fakharani, A., 2017. Geology, structure, geochemistry and ASTER-based mapping of Neoproterozoic Gebel El-Delihimmi granites, Central Eastern Desert of Egypt. Lithos, 282-283, pp. 358-372. https://doi.org/10.1016/j.lithos.2017.03.022

Bifet, A., Gavaldà, R., 2007. Learning from Time-Changing Data with Adaptive Windowing. In: *Proceedings of the 2007 SIAM International Conference on Data Mining*. Society for Industrial and Applied Mathematics, pp. 443–448.

https://doi.org/10.1137/1.9781611972771.42

Brožová, N., Baggio, T., D'Agostino, V., Bühler, Y. and Bebi, P., 2021. *Multiscale analysis of surface roughness for the improvement of natural hazard modelling*. Natural Hazards and Earth System Sciences, 21(11), pp. 3539-3562. https://doi.org/10.5194/nhess-21-3539-2021

Cunha, E.R. and Bacani, V.M., 2016. Morphometric Characterization of a Watershed through SRTM Data and Geoprocessing Technique. Journal of Geographic Information System 8, pp.238-247. http://dx.doi.org/10.4236/jgis.2016.82021

Dell'Acqua, F. and Gamba, P., 2002. *Preparing an urban test site for SRTM data validation*. IEEE Transactions on Geoscience and Remote Sensing, 40(10), pp. 2248–2256. https://doi.org/10.1109/TGRS.2002.802876

Denker, H., 2005. Evaluation of SRTM3 and GTOPO30 Terrain Data in Germany. In: Jekeli, C., Bastos, L., Fernandes, J. (eds), 2005. *Gravity, Geoid and Space Missions*. International Association of Geodesy Symposia, 129, pp.218-223. Springer, Berlin, Heidelberg. https://doi.org/10.1007/3-540-26932-0_38

Dian, Y., Guo, Z., Liu, H., Lin, H., Huang, L., Han, Z., Zhou, M., Cui, H. and Wang, P., 2024. A new index integrating forestry and ecology models for quantitatively characterizing forest carbon sequestration potential ability in a subtropical region. Ecological Indicators, 158, p. 111358. https://doi.org/10.1016/j.ecolind.2023.111358

EL-Omairi, M.A., Garouani, A.E., Shebl, A. Investigation of lineament extraction: Analysis and comparison of digital elevation models in the Ait Semgane region, Morocco. Remote Sensing Applications: Society and Environment, 36, p. 101321. https://doi.org/10.1016/j.rsase.2024.101321

Embrapa – Empresa Brasileira de Pesquisa Agropecuária, 1979. Relevo. In: Serviço Nacional de Levantamento e Conservação de Solos. *Súmula da X reunião técnica de levantamento de solos*. p.27. Rio de Janeiro. Available at: <https://ainfo.cnptia.embrapa.br/digital/bitstream/it

em/212100/1/SNLCS-Miscelania-1-1979.pdf>
[Accessed 10 February 2020].

Esin, A.İ., Akgul, M., Akay, A.O. and Yurtseven, H., 2021. *Comparison of LiDAR-based morphometric analysis of a drainage basin with results obtained from UAV, TOPO, ASTER and SRTM-based DEMs.* Arabian Journal of Geosciences, 14, p. 340.
https://doi.org/10.1007/s12517-021-06705-3

Farr, T.G., Rosen, A.P., Caro, E., Crippen, R., Duren, R., Hensley, S., Kobrick, M., Paller, M., Rodriguez, E., Roth, L., Seal, D., Shaffer, S., Shimada, J., Umland, J., Werner, M., Oskin, M., Burbank, D. and Alsdorf, D., 2007. *The Shuttle Radar Topography Mission.* Reviews of Geophysics, 45(2), pp. 1-33.
https://doi.org/10.1029/2005RG000183

Gomes, J.L.S., 2020. *Morphometric characterization of the Todos os Santos river basin in Minas Gerais – Brazil.* International Journal of Geoscience, Engineering and Technology, 1(1), pp. 1-6. https://doi.org/10.70597/ijget.v1i1.361

Gomes, J.L.S. and Gomes, A.J.L., 2015. *Morfometria do Município de Jenipapo de Minas no Vale do Jequitinhonha.* Vozes dos Vales, (8), pp. 1-15. Available at: <http://site.ufvjm.edu.br/revistamultidisciplinar/files/2015/11/Antonio.pdf> [Accessed 10 February 2024].

Gomes, J.L.S. and Gomes, A.J.L., 2023a. *Mapa Hipsométrico do Município de Jenipapo de Minas.* Geovales. [online] Available at: <https://64950d2b-2638-497b-9aa0-8f3bdf54c4e1.filesusr.com/ugd/3e616a_9d8149e5e900482d93744cb103fedd25.pdf> [Accessed 10 February 2024].

Gomes, J.L.S. and Gomes, A.J.L., 2023b. *Mapa Declividade do Município de Jenipapo de Minas.* Geovales. [online] Available at: <https://64950d2b-2638-497b-9aa0-8f3bdf54c4e1.filesusr.com/ugd/3e616a_d1ae7e4d96e642439a49a61bba3a8513.pdf> [Accessed 15 February 2024].

Gomes, J.L.S., Vieira, F.P. and Hamza, V.M., 2018. *Use of electrical resistivity tomography in selection of sites for underground dams in a semiarid region in southeastern Brazil.* Groundwater for Sustainable Development, 7, pp. 232-238.

https://doi.org/10.1016/j.gsd.2018.06.001

Grohmann, C.H., Riccomini, C. and Steiner, S.S., 2008. SRTM DEMSs applications in Geomorphology. Revista Geográfica Acadêmica, 2(2), pp. 79-83.
https://doi.org/10.31223/osf.io/amn2t

IBGE – Instituto Brasileiro de Geografia e Estatística, 2022a. *Jenipapo de Minas.* Available at: <https://www.ibge.gov.br/cidades-e-estados/mg/jenipapo-de-minas.html> [Accessed 10 September 2024].

IBGE – Instituto Brasileiro de Geografia e Estatística, 2022b. *Malha Municipal.* Available at: <https://www.ibge.gov.br/geociencias/organizacao-do-territorio/malhas-territoriais/15774-malhas.html> [Accessed 10 September 2024].

Jarvis, A., Reuter, H.I., Nelson, A. and Guevara, E., 2008. *Hole-Filled Seamless SRTM Data V4.* International Centre for Tropical Agriculture (CIAT), Cali. Available at: <http://srtm.csi.cgiar.org> [Accessed 10 September 2024].

Lepsch, I.F., Bellinazzi Junior, R., Bertolini, D. and Espíndola, C.R., 1991. *Manual para levantamento utilitário do meio físico e classificação de terras no sistema de capacidade de uso.* Campinas: Sociedade Brasileira de Ciência de Solo.

LaLonde, T., Shortridge, A. and Messina, J., 2010. *The Influence of Land Cover on Shuttle Radar Topography Mission (SRTM) Elevations in Low-relief Areas.* Transactions in GIS, 14(4), pp. 461-479.
https://doi.org/10.1111/j.1467-9671.2010.01217.x

Listyani, T.R.A., 2019. *Criticise of Van Zuidam Classification: A Purpose of Landform Unit.* Prosiding Nasional Rekayasa Teknologi Industri dan Informasi (ReTII), XIV, pp.332-337.

Liu, Z., Zhu, J., Fu, H., Zhou, C. and Zuo, T., 2020. *Evaluation of the Vertical Accuracy of Open Global DEMs over Steep Terrain Regions Using ICESat Data: A Case Study over Hunan Province, China.* Sensors, 20(17), pp. 1-16.
https://doi.org/10.3390/s20174865

Moudrý, V., Lecours, V., Gdulová, K., Gábor, L., Moudrá, L., Kropáček, J., and Wild, J., 2018. On the use of global DEMs in ecological modelling and the accuracy of new bare-earth DEMs. Ecological Modelling, 383, pp. 3-9.
https://doi.org/10.1016/j.ecolmodel.2018.05.006

Nikolakopoulos, K.G., Kamaratakis, E.K. and Chrysoulakis, N., 2006. *SRTM vs. ASTER Elevation Products. Comparison for Two Regions in Crete, Greece.* International Journal of Remote Sensing, 27, pp. 4819-4838.
https://doi.org/10.1080/01431160600835853

Okolie, C.J. and Smit, J.L., 2022. *A systematic review and meta-analysis of Digital elevation model (DEM) fusion: pre-processing, methods and applications.* ISPRS Journal of Photogrammetry and Remote Sensing, 188, pp. 1-29.
https://doi.org/10.1016/j.isprsjprs.2022.03.016

Ouerghi, S., ELsheikh, R.F.A., Achour, H. and Bouazi, S., 2015. *Evaluation and Validation of Recent Freely-Available ASTER-GDEM V.2, SRTM V.4.1 and the DEM Derived from Topographical Map over SW Grombalia (Test Area) in North East of Tunisia.* Journal of Geographic Information System, 7, pp. 266-279.
http://dx.doi.org/10.4236/jgis.2015.73021

Passini, R., Jacobsen, K., 2007. High Resolution SRTM Height Models: In: The International Archives of the Photogrammetry, Remote Sensing and Spatial Information Sciences (IntArchPhRS XXXVI), 36. Band 1/W51. Hannover. Available at: <https://www.isprs.org/proceedings/xxxvi/1-w51/paper/Passini_jac.pdf> [Accessed 10 September 2024].

Riley, S.J., DeGloria, S.D., Elliott, R., 1999. *A terrain ruggedness index that quantifies topographic heterogeneity.* Intermountain Journal of Sciences, 5(1-4), pp. 23-27. Available at: <https://download.osgeo.org/qgis/doc/reference-docs/Terrain_Ruggedness_Index.pdf> [Accessed 10 September 2024].

Rodríguez, E., Morris, C. and Belz, J.E., 2006. *A global assessment of the SRTM performance.* Photogrammetric Engineering and Remote Sensing, 72(3), pp. 249-60.
https://doi.org/10.14358/PERS.72.3.249

Rossetti, D.F. and Valeriano, M.M., 2007. Evolution of the lowest amazon basin modeled from the integration of geological and SRTM topographic data. CATENA, 70(2), pp. 253-265.
https://doi.org/10.1016/j.catena.2006.08.009

Shen, L., Wei, Z., Wang, Y., 2021. *Determining the Rolling Window Size of Deep Neural Network Based Models on Time Series Forecasting.* Journal of Physics: Conference Series, 2078.
https://doi.org/10.1088/1742-6596/2078/1/012011

Silva, A.C., Gomes, J.L.S. and Oliveira, V.P.S., 2023. Identificação dos diferentes usos e ocupação do solo na Reserva Ecológica de Guapiaçu (REGUA) com vista à sustentabilidade. In: Simpósio de Gestão Ambiental e Biodiversidade (SIGABI), 12. 2023, Três Rios(RJ) UFRRJ.
http://dx.doi.org/10.29327/1326957.12-2

Suwandana, E., Kawamura, K., Sakuno, Y. and Kustiyanto, E., 2011. *Thematic information content assessment of the ASTER GDEM: a case study of watershed delineation in West Java, Indonesia.* Remote Sensing Letters, 3(5), pp. 423–432.
https://doi.org/10.1080/01431161.2011.593580

Thakuri, S., Parajuli, B.P., Shakya, P., Baskota, P., Pradhan, D., Chauhan, R., 2022. *Open-Source Data Alternatives and Models for Flood Risk Management in Nepal.* Remote Sensing, 14(22), pp.1-28.
https://doi.org/10.3390/rs14225660

Thomas, J., Joseph, S., Thrivikramji, K.P. and Arunkumar, K.S., 2014. *Sensitivity of digital elevation models: The scenario from two tropical mountain river basins of the Western Ghats, India.* Geoscience Frontiers, 5(6), pp. 893-909.
https://doi.org/10.1016/j.gsf.2013.12.008

Trevisani, S., Teza, G. and Guth, P.J., 2023. *Hacking the topographic ruggedness index.* Geomorphology, 439, p. 108838.
https://doi.org/10.1016/j.geomorph.2023.108838

Uuemaa, E., Ahi, S., Montibeller, B., Muru, M., Kmoch, A., 2020. *Vertical Accuracy of Freely Available Global Digital Elevation Models (ASTER, AW3D30, MERIT, TanDEM-X, SRTM, and NASADEM).* Remote Sensing, 12(21), p. 3482.

https://doi.org/10.3390/rs12213482

Van Zyl, J.J., 2001. The Shuttle Radar Topography Mission (SRTM): a breakthrough in remote sensing of topography. Acta Astronautica, 48(5-12), pp. 559–565.
https://doi.org/10.1016/S0094-5765(01)00020-0

Van Zuidam, R.A., 1983. *Guide to Geomorphologic Aerial Photographic Interpretation & Mapping*. Netherlands: International Institute for Aerial Survey and Earth Sciences (ITC).

Van Zuidam, R.A. and Van Zuidam-Cancelado, F.I., 1979. *Terrain Analysis and Classification using Aerial Photographs*. Tectbook VII-6, Netherland: International Institute for Aerial Survey and Earth Sciences (ITC).